

# 96 GeV Scalar Boson in the 2HDM with $U(1)_H$ Gauge Symmetry

---

Seungwon Baek,<sup>a</sup> P. Ko,<sup>b,c</sup> Yuji Omura<sup>d</sup> and Chaehyun Yu<sup>e</sup>

<sup>a</sup>*The Institute of Basic Science, Korea University, Anam-ro 145, Seoul 02841, Korea*

<sup>b</sup>*School of Physics, Korea Institute for Advanced Study (KIAS), 85 Hoegi-ro, Seoul 02455, Korea*

<sup>c</sup>*Quantum Universe Center (QUC), KIAS, 85 Hoegi-ro, Seoul 02455, Korea*

<sup>d</sup>*Department of Physics, Kindai University, Higashi-Osaka, Osaka 577-8502, Japan*

<sup>e</sup>*Department of Physics Education and RINS, Gyeongsang National University, Jinju 52828, Korea*

In this paper, we study two Higgs doublet models with gauged  $U(1)_H$  symmetry, motivated by the excesses around 96 GeV reported by the CMS collaboration in the searches for light resonances decaying to two photons and two  $\tau$ 's. In this model, one Higgs doublet field is charged under the  $U(1)_H$  symmetry to avoid tree-level flavor changing neutral currents. The extra gauge symmetry requires extra chiral fermions, to satisfy the anomaly-free conditions. We analyze the signals of the light resonances, taking into account the contribution of the extra fermions, and discuss the consistency with the experimental results in this model.

---

## Contents

<b>1</b>	<b>Introduction</b>	<b>1</b>
<b>2</b>	<b>The 2HDM with gauged <math>U(1)_H</math> symmetry</b>	<b>3</b>
<b>3</b>	<b>Constraints</b>	<b>7</b>
3.1	Theoretical constraints	7
3.2	Electroweak precision observables	8
3.3	Flavor physics	9
3.4	Experiments for scalar bosons	9
<b>4</b>	<b>Results</b>	<b>9</b>
4.1	Parameters	9
4.2	Analysis	11
4.3	Constraints from $t\bar{t}\tau^+\tau^-$ production at the LHC	13
4.4	Benchmark points	14
<b>5</b>	<b>Summary</b>	<b>14</b>
<b>A</b>	<b>Bounded-from-below condition</b>	<b>15</b>
<b>B</b>	<b>Effective couplings</b>	<b>16</b>

---

## 1 Introduction

The Standard Model (SM) has been established as a theory describing particle physics. Almost all predictions of the SM are consistent with experimental results and the Higgs particle was finally discovered at the LHC [1, 2]. It is certain that there are still large uncertainties in some observables, so that new physics may exist in the energy region that can be explored at the LHC. The new model, however, should not drastically modify the SM predictions. A lot of candidates for new physics have been proposed, motivated by problems in the SM. The mysteries, especially, concerned with the origin of the electroweak (EW) scale and the vacuum structure of our universe seems to suggest new particles around the EW scale. Thus, some extensions of the SM model that reveals new aspects of our universe may be confirmed near future.

Recently, the CMS collaboration has reported some excesses in the diphoton channel around 96 GeV mass region, that may suggest interesting possibilities of the vacuum structure. The CMS collaboration has surveyed resonances that decay to two photons, and reported deviations from the expected signals. Based on the data at  $\sqrt{s} = 8$  TeV and 13 TeV with the integrated luminosity of  $19.7 \text{ fb}^{-1}$  and  $35.9 \text{ fb}^{-1}$ , respectively, the result shows

a resonance at 95.3 GeV with a local significance of  $2.8\sigma$ . This can be described by a signal strength, [3]

$$\mu_{\gamma\gamma}^{\text{CMS,previous}} = \frac{\sigma^{\text{exp}}(gg \rightarrow s \rightarrow \gamma\gamma)}{\sigma^{\text{SM}}(gg \rightarrow H^{\text{SM-like}} \rightarrow \gamma\gamma)} = 0.6 \pm 0.2. \quad (1.1)$$

Here  $s$  denotes the 96 GeV scalar boson responsible for the resonance while the  $H^{\text{SM-like}}$  is the hypothetical Higgs boson with the mass for the resonance. The analysis with full data Run 2 data set has been already reported by the CMS collaboration. The result shows an excess with a local significance of  $2.9\sigma$  at 95.4 GeV. This signal strength for the resonance is [4]

$$\mu_{\gamma\gamma}^{\text{CMS}} = \frac{\sigma^{\text{exp}}(gg \rightarrow s \rightarrow \gamma\gamma)}{\sigma^{\text{SM}}(gg \rightarrow H^{\text{SM-like}} \rightarrow \gamma\gamma)} = 0.33_{-0.12}^{+0.19}. \quad (1.2)$$

The ATLAS collaboration has also reported their analysis for the di-photon channel with the full Run 2 data set and found a mild excess with a local significance of  $1.7\sigma$  [5] which corresponds to the signal strength of [6]

$$\mu_{\gamma\gamma}^{\text{ATLAS}} = 0.18_{-0.10}^{+0.10}. \quad (1.3)$$

The combined signal strength of the CMS and ATLAS results without possible correlation is [6]

$$\mu_{\gamma\gamma}^{\text{exp}} = 0.24_{-0.08}^{+0.09} \quad (1.4)$$

at the mass of 95.4 GeV. The CMS collaboration has also reported another resonance which may be a candidate for an extra scalar boson in the di- $\tau$  channel. The local significance at 95 GeV is about  $2.6\sigma$  and the corresponding signal strength is [7]

$$\mu_{\tau\tau}^{\text{CMS}} = \frac{\sigma^{\text{exp}}(gg \rightarrow s \rightarrow \tau\tau)}{\sigma^{\text{SM}}(gg \rightarrow H^{\text{SM-like}} \rightarrow \tau\tau)} = 1.2 \pm 0.5, \quad (1.5)$$

while there has been no analysis at ATLAS for the corresponding region so far. In addition, the LEP collaboration has announced a resonance at a similar invariant mass of a  $b\bar{b}$  pair. The resonance in the  $e^+e^- \rightarrow Zs \rightarrow Zb\bar{b}$  channel was observed with a local significance of  $2.3\sigma$ . The excess can be interpreted as the signal strength of [8, 9]

$$\mu_{b\bar{b}}^{\text{LEP}} = \frac{\sigma^{\text{exp}}(e^+e^- \rightarrow Z(s \rightarrow b\bar{b}))}{\sigma^{\text{SM}}(e^+e^- \rightarrow Z(H^{\text{SM-like}} \rightarrow b\bar{b}))} = 0.117 \pm 0.057, \quad (1.6)$$

where the mass of the resonance is about 98 GeV.

If those deviations are originated from new resonances that reside around 96 GeV, one of the good candidates is a neutral scalar originated from scalar fields that contribute to the EW symmetry breaking [6, 10–18]. The possibility that extra scalar fields may exist has been discussed in many works. Adding extra scalar fields is surely one simple way to extend the SM without disturbing the anomaly-free conditions. Scalar fields may play a role in breaking extra gauge symmetries. In fact, extra neutral scalars that are related to gauge symmetry breaking and reside around 96 GeV have been proposed motivated by the excesses, and the signals have been studied in many works [19–49].

One of the simple extensions of the SM with extra scalar fields contributing to the EW symmetry breaking is two Higgs doublet models (2HDMs). In generic 2HDMs, both of the Higgs doublets can contribute simultaneously to fermion masses when they develop nonzero vacuum expectation values (VEVs). Since the fermion mass matrices and Yukawa couplings are not simultaneously diagonalizable, Higgs mediated flavor-changing neutral currents (FCNCs) will be present even at tree levels. Then a large portion of the parameter space in the generic 2HDMs would have already been excluded by stringent constraints from flavor physics such as  $M^0 - \overline{M^0}$  mixings (with  $M = K, B_d, B_s$ ),  $B \rightarrow X_s \gamma$ ,  $B_s \rightarrow \mu^+ \mu^-$ ,  $l \rightarrow l' \gamma$ ,  $l \rightarrow 3l'$  etc., to name a few.

The Higgs-mediated FCNC problem in generic 2HDMs can be cured *a la* by Natural Flavor Conservation Criterion by Glashow and Weinberg [50]. A simple realization of their criterion is to introduce  $Z_2$  symmetry under which two Higgs doublets are different  $Z_2$  parity. Then the SM chiral fermions will also carry different  $Z_2$  charges. There are four different charge assignments for which Yukawa couplings of the SM fermions are allowed in such a way that the fermions of the same electric charge gets their masses from one and the same Higgs doublet, either  $H_1$  or  $H_2$ , but not from both. Namely 2HDMs that do not predict tree level FCNCs are classified into four types. In the Type-I 2HDM, only one Higgs field is coupled to the SM fermions. In the Type-II 2HDM, one Higgs field ( $H_1$ ) couples with right-handed down-type quarks and charged leptons, and the other Higgs field ( $H_2$ ) couples with right-handed up-type quarks and neutrinos. It is possible to consider a model where the couplings are flipped:  $H_1$  couples with right-handed down-type quarks and neutrinos, and the  $H_2$  couples with right-handed up-type quarks and charged leptons. We call this model the Type-Y 2HDM. In the fourth 2HDM,  $H_1$  couples with quarks and  $H_2$  couples with leptons. Then this  $Z_2$  symmetry is assumed to be softly broken by dim-2 operator,  $m_{12}^2 H_1^\dagger H_2 + H.c.$ , in order to increase the masses of the scalars originated from  $H_1$  and  $H_2$ .

In this paper, we consider gauged  $U(1)_H$  symmetry instead of softly broken  $Z_2$  symmetry, by assigning a non-vanishing  $U(1)_H$  charge to  $H_2$  [51–54]. In addition, extra complex singlet scalar field,  $\Phi$ , is also introduced in order to break  $U(1)_H$  spontaneously. As discussed in Ref. [51], there are several possible setups in 2HDMs with gauged  $U(1)_H$ . In this work, we concentrate on the Type-II 2HDM and the Type-Y 2HDM motivated by the excesses around 96 GeV. In Sec. 2, we discuss the setups of our 2HDMs. In Sec. 3, we summarize experimental constraints relevant to our models. In Sec. 4, the analyses concerned with the excesses are shown. Sec. 5 is devoted to summary. In Appendix A, the constraints from the condition for the scalar potential to be bounded from below is introduced. In Appendix B, the relevant effective couplings are summarized.

## 2 The 2HDM with gauged $U(1)_H$ symmetry

We consider 2HDMs with extra  $U(1)_H$  gauge symmetry, where one of the Higgs field  $H_2$  is charged under the  $U(1)_H$  gauge symmetry, while the other  $H_1$  is not charged. Some SM fermions may be also charged under  $U(1)_H$  so that phenomenologically viable Yukawa

couplings for the SM fermions are allowed by the presumed gauge symmetry. Below, we discuss the detail based on Refs. [51–54].

Due to the charge assignment to the scalar doublet fields, both  $H_1^\dagger H_2$  and  $(H_1^\dagger H_2)^2$  terms are forbidden in the model. It has been found that this setup for the scalar potential is not excluded by experiments so far [55]. However, because there is no new scale in the potential, the masses of the new scalar bosons in the model, in particular, the mass of the charged Higgs boson, are of at most EW scale of the VEV  $v \sim 246$  GeV. We add a new singlet scalar field  $\Phi$  to the model, which gives rise to the  $H_1^\dagger H_2$  term after symmetry breaking. Then both the charged Higgs and extra neutral Higgs bosons can be heavier than the SM Higgs boson.

	$H_1$	$H_2$	$\Phi$
$SU(3)_c$	<b>1</b>	<b>1</b>	<b>1</b>
$SU(2)$	<b>2</b>	<b>2</b>	<b>1</b>
$U(1)_Y$	1/2	1/2	0
$U(1)_H$	0	1	-1

**Table 1.** The charge assignment to the scalar fields.

The charge assignments under  $G_{SM} \times U(1)_H$  gauge symmetry to the scalar fields are shown in Table 1. Then the renormalizable parts of the scalar potential in our model is

$$V(H_k, \Phi) = m_k^2 H_k^\dagger H_k + \lambda_k (H_k^\dagger H_k)^2 + \lambda_3 (H_1^\dagger H_1)(H_2^\dagger H_2) + \lambda_4 |H_1^\dagger H_2|^2 + m_\Phi^2 |\Phi|^2 + \lambda_\Phi |\Phi|^4 + \tilde{\lambda}_k |\Phi|^2 H_k^\dagger H_k - \left\{ \sqrt{2} \mu_\Phi H_1^\dagger H_2 \Phi + H.c. \right\}, \quad (2.1)$$

where  $k = 1, 2$ . We emphasize that, compared to the usual 2HDMs, two operators are missing in our model due to the  $U(1)_H$  gauge symmetry: the soft  $Z_2$  breaking dim-2 operator,  $m_{12}^2 H_1^\dagger H_2$ , and the  $\lambda_5 (H_1^\dagger H_2)^2 + h.c.$  term. Still the  $H_1^\dagger H_2 + h.c.$  term can be realized from the  $H_1^\dagger H_2 \Phi + h.c.$  terms after the singlet field  $\Phi$  develops a non-vanishing VEV.

The scalar fields are expanded around nonzero VEVs with only  $SU(3)_C \times U(1)_{em}$  remaining unbroken:

$$\langle H_k \rangle = (0, v_k / \sqrt{2})^\top, \quad \langle \Phi \rangle = v_\Phi / \sqrt{2}, \quad (2.2)$$

and

$$H_k = \begin{pmatrix} \phi_k^+ \\ \frac{v_k}{\sqrt{2}} + \frac{1}{\sqrt{2}}(h_k + i\chi_k^0) \end{pmatrix}, \quad \Phi = \frac{1}{\sqrt{2}}(v_\Phi + h_\Phi + i\chi_\Phi), \quad (2.3)$$

where  $v_1 = v \cos \beta$ ,  $v_2 = v \sin \beta$ , and  $v = \sqrt{v_1^2 + v_2^2} = 246$  GeV.

After the electroweak (EW) and  $U(1)_H$  gauge symmetry breaking, three CP-even neutral scalar fields,  $h_i \equiv (h_1, h_2, h_\Phi)$ , mix among themselves, and the  $3 \times 3$  mass matrix is diagonalized by three physical states,  $S_i \equiv (\tilde{h}, h, H)$ .  $h$  is identified as the Higgs boson with the mass of 125 GeV while  $\tilde{h}$  is as the 96 GeV scalar boson. The remaining  $H$  is an additional scalar boson. The mixing between three scalar bosons are defined by

$$S_i = R_{ij} h_j, \quad (2.4)$$

where the rotation matrix  $R_{ij}$  is given by

$$R = \begin{pmatrix} 1 & 0 & 0 \\ 0 & \cos \alpha_3 & \sin \alpha_3 \\ 0 & -\sin \alpha_3 & \cos \alpha_3 \end{pmatrix} \begin{pmatrix} \cos \alpha_2 & 0 & \sin \alpha_2 \\ 0 & 1 & 0 \\ -\sin \alpha_2 & 0 & \cos \alpha_2 \end{pmatrix} \begin{pmatrix} \cos \alpha_1 & \sin \alpha_1 & 0 \\ -\sin \alpha_1 & \cos \alpha_1 & 0 \\ 0 & 0 & 1 \end{pmatrix} \quad (2.5)$$

with three mixing angles,  $\alpha_i$  ( $i = 1, 2, 3$ ).

The CP-odd states,  $\chi = (\chi_\Phi, \chi_1, \chi_2)$ , also mix among themselves and yield two Nambu-Goldstone bosons,  $G_1^0$  and  $G_2^0$ , and one pseudoscalar boson,  $A$ . The mixing angles are defined by  $G_i = (V_A)_{ij}\chi_j$ , where  $G = (G_1^0, G_2^0, A)$  and

$$V_A = \begin{pmatrix} 0 & \cos \beta & \sin \beta \\ \cos \delta & \sin \beta \sin \delta & -\cos \beta \sin \delta \\ \sin \delta & -\sin \beta \cos \delta & \cos \beta \cos \delta \end{pmatrix} \quad (2.6)$$

with

$$\cos \delta = \frac{v_\Phi}{\sqrt{v_\Phi^2 + (v \cos \beta \sin \beta)^2}}. \quad (2.7)$$

Then the mass of the pseudoscalar boson is obtained by the mixing matrix as

$$m_A^2 = \mu_\Phi \left( \frac{v_1 v_\Phi}{v_2} + \frac{v_1 v_2}{v_\Phi} + \frac{v_2 v_\Phi}{v_1} \right). \quad (2.8)$$

The three neutral gauge bosons mix among them after EW and  $U(1)_H$  symmetry breaking, and their mass matrix is given by

$$M^2 = \frac{v^2}{8} \begin{pmatrix} g^2 & -gg_Y^2 & -2gg_X s_\beta^2 \\ -gg_Y & g_Y^2 & 2g_Y g_X s_\beta^2 \\ -2gg_X s_\beta^2 & 2g_Y g_X s_\beta^2 & 4g_X^2 \left( s_\beta^2 + \frac{v_\Phi^2}{v^2} \right) \end{pmatrix}, \quad (2.9)$$

where  $g, g_Y$ , and  $g_X$  are gauge couplings for  $U(1)_Y, SU(2)_L$ , and  $U(1)_H$ , respectively, and  $s_\beta = \sin \beta$ . A massless state is identified as the photon and the remaining two states mix with each other. Then the two massive bosons,  $Z$  and  $Z'$ , are expressed as

$$\hat{Z} = Z \cos \theta + Z' \sin \theta, \quad (2.10)$$

$$\hat{Z}' = Z \sin \theta - Z' \cos \theta, \quad (2.11)$$

where the  $\hat{Z}$  and  $\hat{Z}'$  are two states after identifying the photon state. The mixing angle is defined by

$$\sin \theta = \frac{\lambda}{(1 + \lambda^2)^{1/2}}, \quad (2.12)$$

where

$$\lambda = \frac{\bar{g}^2 - g_H^2 + [(\bar{g}^2 - g_H^2)^2 + 4\bar{g}^2 \bar{\delta}^2]^{1/2}}{2\bar{g}\bar{\delta}}, \quad (2.13)$$

$$\bar{g}^2 = g_Y^2 + g^2, \quad (2.14)$$

$$g_H^2 = 4g_X^2 \left( s_\beta^2 + \frac{v_\Phi^2}{v^2} \right), \quad (2.15)$$

$$\bar{\delta} = 2g_X s_\beta^2. \quad (2.16)$$

	$Q_L^i$	$u_R^i$	$d_R^i$	$L_L^i$	$e_R^i$	$\nu_R^i$
$SU(3)_c$	<b>3</b>	<b>3</b>	<b>3</b>	<b>1</b>	<b>1</b>	<b>1</b>
$SU(2)$	<b>2</b>	<b>1</b>	<b>1</b>	<b>2</b>	<b>1</b>	<b>1</b>
$U(1)_Y$	1/6	2/3	-1/3	-1/2	-1	0
$U(1)_H$	-1/3	2/3	-1/3	0	0	1

**Table 2.** The charge assignment to the SM fermions in the Type-II 2HDM.

	$Q_L^i$	$u_R^i$	$d_R^i$	$L_L^i$	$e_R^i$	$\nu_R^i$
$SU(3)_c$	<b>3</b>	<b>3</b>	<b>3</b>	<b>1</b>	<b>1</b>	<b>1</b>
$SU(2)$	<b>2</b>	<b>1</b>	<b>1</b>	<b>2</b>	<b>1</b>	<b>1</b>
$U(1)_Y$	1/6	2/3	-1/3	-1/2	-1	0
$U(1)_H$	0	1	0	0	-1	0

**Table 3.** The charge assignment to the SM fermions in the Type-Y 2HDM.

The fermion sector depends on the  $U(1)_H$  charge assignments to the SM fermions. It turns out that the Type-I 2HDM for the fermions can be constructed by adding right-handed neutrinos without any gauge anomalies [51–53], while models of other types require extra fermions as well as right-handed neutrinos in order to cancel gauge anomalies [51, 54]. In this paper we focus on the Type-II and Type-Y models which are relevant to the 96GeV scalar resonance signals [10]. In Tables 2 and 3, we show the  $U(1)_H$  charge assignments to the SM fermions in the Type-II and Type-Y 2HDMs, respectively.

Then we obtain the same Yukawa interactions as those in the usual 2HDM in both types. In the Type-II 2HDM, the Yukawa interaction is

$$\mathcal{L}_{\text{Yukawa}}^{II} = -Y_u^{ij} \overline{Q}_L^i \tilde{H}_2 u_R^j - Y_d^{ij} \overline{Q}_L^i H_1 d_R^j - Y_e^{ij} \overline{L}_L^i H_1 e_R^j - Y_n^{ij} \overline{L}_L^i \tilde{H}_2 \nu_R^j + h.c., \quad (2.17)$$

while in the Type-Y 2HDM the Yukawa interaction is given by

$$\mathcal{L}_{\text{Yukawa}}^Y = -Y_u^{ij} \overline{Q}_L^i \tilde{H}_2 u_R^j - Y_d^{ij} \overline{Q}_L^i H_1 d_R^j - Y_e^{ij} \overline{L}_L^i H_2 e_R^j - Y_n^{ij} \overline{L}_L^i \tilde{H}_1 \nu_R^j + h.c., \quad (2.18)$$

where,  $\tilde{H}_{1,2} = i\sigma_2 H_{1,2}^*$  and  $i, j = 1, 2, 3$ .

In both models, the gauge anomalies involving  $U(1)_H$  currents are not cancelled with SM fermions only, and additional new chiral fermions have to be introduced in order to fulfill the anomaly cancellation conditions. We could find a lot of setups without gauge anomaly [51]. The Type-II 2HDM, for instance, can be realized by the model inspired by the  $E_6$  Grand Unified Theory [54]. The anomaly-free conditions in the Type-Y 2HDM can be satisfied, by adding extra quarks and leptons in Table 4 when the  $U(1)_H$  charge assignments to the SM fermions are as in Table 3. Note that Yukawa couplings between  $\Phi$  and extra fermions are allowed by the assumed gauge symmetries:

$$\mathcal{L}_{\text{extra}}^Y = -y_D^i \overline{u_L^i} \Phi^\dagger u_R^i - y_L^i \overline{e_L^i} \Phi e^i + h.c.. \quad (2.19)$$

In this paper, we do not pay attention to the extra fermions too much because they strongly

	$u_L^i$	$u_R^i$	$e_L^i$	$e_R^i$
$SU(3)_c$	<b>3</b>	<b>3</b>	<b>1</b>	<b>1</b>
$SU(2)$	<b>1</b>	<b>1</b>	<b>1</b>	<b>1</b>
$U(1)_Y$	2/3	2/3	-1	-1
$U(1)_H$	1	0	-1	0

**Table 4.** The charge assignment to the extra fermions in the Type-Y model.

depends on the model construction which is not unique. Our motivation is to study the effects of the extra fermions to the scalar boson decays such as  $\tilde{h} \rightarrow \gamma\gamma$  through the loops. Thus the extra fermion contributions to the loop diagrams must be considered collectively, that is the sum of all the fermions in the model, which is quite cumbersome. Instead, we assume a vectorlike charged lepton and quark as a representative of collection of the extra fermions in the loop, denoting the Yukawa couplings of extra quarks and leptons as  $y_D$  and  $y_L$ , respectively. In our phenomenological analysis, those parameters are fixed at  $y_D = y_L = 1$ .

### 3 Constraints

In this section, we consider various theoretical and phenomenological constraints on our models.

#### 3.1 Theoretical constraints

First, we consider the constraints from the vacuum stability conditions for nonzero VEVs. The requirement for the scalar potential to be stable and bounded from below constrain the dimensionless couplings in the scalar potential. Following the approach in Ref. [56], we find the constraints on the dimensionless couplings, which are presented in appendix A.

The models also have constraints from perturbative unitarity bounds. Following the method to find the constraints from perturbative unitarity [57, 58], we find that the constraints are given by

$$|b_{\pm}|, |c_{\pm}|, |f_{\pm}|, |g_{\pm}|, |f_{s,s_1,s_2}|, \frac{1}{2}|a_{1,2,3}| \leq 8\pi, \quad (3.1)$$

where

$$\begin{aligned} b_{\pm} &= 2\lambda_{1,2}, & c_{\pm} &= \lambda_1 + \lambda_2 \pm \sqrt{(\lambda_1 - \lambda_2)^2 + \lambda_4^2}, \\ f_{\pm} &= \lambda_3 + \lambda_4 \pm \lambda_4, & g_{\pm} &= \lambda \pm \lambda_4, \\ f_s &= 2\lambda_{\Phi}, & f_{s_1} &= \tilde{\lambda}_1, & f_{s_2} &= \tilde{\lambda}_2, \end{aligned} \quad (3.2)$$

and  $a_{1,2,3}$  are roots of the cubic equation for  $x$ :

$$\begin{aligned} 0 &= x^3 - 4(3\lambda_1 + 3\lambda_2 + 2\lambda_{\Phi})x^2 \\ &- 4(2\tilde{\lambda}_1^2 + 2\tilde{\lambda}_2^2 + 36\lambda_1\lambda_2 - 4\lambda_3^2 - 4\lambda_3\lambda_4 - \lambda_4^2 + 24\lambda_1\lambda_{\Phi} + 24\lambda_2\lambda_{\Phi})x \\ &+ 96\tilde{\lambda}_1^2\lambda_2 + 96\tilde{\lambda}_2^2\lambda_1 - 64\tilde{\lambda}_1\tilde{\lambda}_2\lambda_3 - 1152\lambda_1\lambda_2\lambda_{\Phi} + 128\lambda_3^2\lambda_{\Phi} + 128\lambda_3\lambda_4\lambda_{\Phi} + 32\lambda_4^2\lambda_{\Phi}. \end{aligned}$$



### 3.2 Electroweak precision observables

In order to study the physical effects on the electroweak precision observables (EWPOs) in this model, full calculations of the relevant amplitudes at the one-loop level is required, which is quite involved. Instead we calculate the  $\Delta T$  parameter approximately. Due to the  $Z$ - $Z'$  mixing, the mass of the  $Z$  boson is shifted

$$m_Z^2 = \frac{m_W^2}{c_W^2} \cos^2 \theta - m_{Z'}^2 \frac{\sin^2 \theta}{\cos^2 \theta}, \quad (3.3)$$

at tree level. We note that the  $W^\pm$  mass is not shifted by the  $U(1)_H$  gauge symmetry. Since the mixing angle is expected to be small, this mass shift changes the  $\rho$  parameter

$$\Delta\rho_\theta = 1 - \frac{1}{\rho} \approx -\sin^2 \theta \left( 1 - \frac{c_W^2 m_{Z'}^2}{m_W^2} \right) \quad (3.4)$$

up to the leading order of  $s_\theta$ . This is converted to the  $T$  parameter as  $T_\theta = \Delta\rho_\theta/\alpha(m_Z)$ .

The new scalar bosons also contribute to the shift of the  $\rho$  parameter at loop levels. At one-loop level, we find that the approximate formula of the contribution is [59]

$$\begin{aligned} T_s = \frac{1}{16\pi m_W^2 s_W^2} & \left[ g_{W^\pm H^\mp A}^2 F(m_{H^\pm}^2, m_A^2) + \sum_i g_{W^\pm H^\mp S_i}^2 F(m_{H^\pm}^2, m_{S_i}^2) \right. \\ & - \sum_i g_{Z A S_i}^2 F(m_A^2, m_{S_i}^2) + 3 \sum_i g_{Z Z S_i}^2 F(m_Z^2, m_{S_i}^2) \\ & - 3 \sum_i g_{W W S_i}^2 F(m_W^2, m_{S_i}^2) + 3 \sum_i g_{Z Z' S_i}^2 F(m_{Z'}^2, m_{S_i}^2) \\ & - 3g_{W^\pm H^\mp Z'}^2 F(m_{Z'}^2, m_{H^\pm}^2) - 3g_{W^\pm H^\mp Z}^2 F(m_Z^2, m_{H^\pm}^2) \\ & \left. - 3F(m_Z^2, m_h^2) + 3F(m_W^2, m_h^2) \right], \quad (3.5) \end{aligned}$$

where the loop function  $F(x, y)$  is defined by

$$F(x, y) = \frac{x+y}{2} - \frac{xy}{x-y} \ln \frac{x}{y} \quad (3.6)$$

for  $x \neq y$  while  $F(x, y) = 0$  for  $x = y$ . The effective couplings,  $g_{W^\pm H^\mp A}$  and so on, are defined in Appendix B. This loop contribution to  $T$  in the case of 2HDMs with  $Z_2$  symmetry vanishes. However, in our model, the EW symmetry breaking makes the  $Z'$  boson massive by absorbing one of degrees of freedom in the scalar fields. Therefore, the presence of the  $U(1)_H$  gauge symmetry implies that the contribution from the  $Z$ - $Z'$  mixing must be taken into consideration together with the scalar loop corrections. Finally, the sum of two contributions leads to

$$T = T_\theta + T_s, \quad (3.7)$$

where the measured value is [60]

$$T^{\text{exp}} = 0.09 \pm 0.07. \quad (3.8)$$

We constrain the  $T$  parameter within  $2\sigma$ .

### 3.3 Flavor physics

The charged Higgs boson mass  $m_{H^\pm}$  and  $\tan\beta$  are strongly constrained by flavor physics, in particular, the  $b \rightarrow s\gamma$  decay. The constraints on the 2HDMs from flavor physics including the experimental results at the LHC were analyzed in Ref. [61]. The constraints on the charged Higgs boson mass and  $\tan\beta$  are the same as those in the 2HDMs. Thus, we take the lower bound of the charged Higgs boson mass to be 600 GeV and set the bound on  $\tan\beta$  from 1 to 3 depending on the charged Higgs boson mass.

### 3.4 Experiments for scalar bosons

There have been a lot of searches for new scalar bosons at the LEP, Tevatron, and LHC, and lots of data have been accumulated. However, there is no definite signal for a new scalar boson so far. These search data except for the resonance data around 96 GeV will strongly constrain our model. We apply these experimental constraints for the additional scalar bosons using the public code `HiggsBounds` [62] where the exclusion limit is 95% C.L..

In our model, the 125 GeV scalar boson will mix with other neutral scalar bosons. Therefore, this mixing changes the predictions for the properties of the observed Higgs boson. Then the precision observables for productions and decays of the 125 GeV Higgs boson also constrain our model strongly. We use the public code `HiggsSignals` [63] to test the 125 GeV Higgs boson in our model. The code performs a  $\chi^2$  test for signal and decay rates of the 125 GeV Higgs boson against the prediction in the SM. Then we put the condition that the p-value evaluated from `HiggsSignals` is less than 0.05.

## 4 Results

In this section, we analyze the resonance signals in both the Type-II 2HDM and the Type-Y 2HDM.

### 4.1 Parameters

In our model, there are 11 parameters as follows:

$$\alpha_1, \alpha_2, \alpha_3, \tan\beta, v_\Phi, m_H, m_A, m_{H^\pm}, y_D, y_L, g_X, \quad (4.1)$$

which denote three mixing angles between CP-even neutral Higgs bosons,  $v_2/v_1$ , the VEV of  $\Phi$ , the heavy neutral Higgs boson mass, the pseudoscalar boson mass, the charged Higgs boson mass, the Yukawa couplings of extra quark and lepton, and the gauge coupling of the  $U(1)_H$  symmetry, respectively.

For the three mixing angles, we allow the entire range,  $0 \leq \alpha_{1,2,3} \leq 2\pi$ . For  $\tan\beta$  and  $v_\Phi$ , we use the following ranges

$$1 \leq \tan\beta \leq 100 \quad \text{and} \quad 1 \leq v_\Phi/\text{GeV} \leq 10^4. \quad (4.2)$$

However, it turns out that  $1 \leq \tan\beta \leq 10$  and  $5 \times 10^3 \leq v_\Phi/\text{GeV} \leq 10^4$  are sufficient for the scanning of the parameters. The ranges of the masses of the extra scalar bosons are taken to be  $10 \leq m_{H,A,H^\pm}/\text{GeV} \leq 1000$ , respectively. The Yukawa couplings of the extra

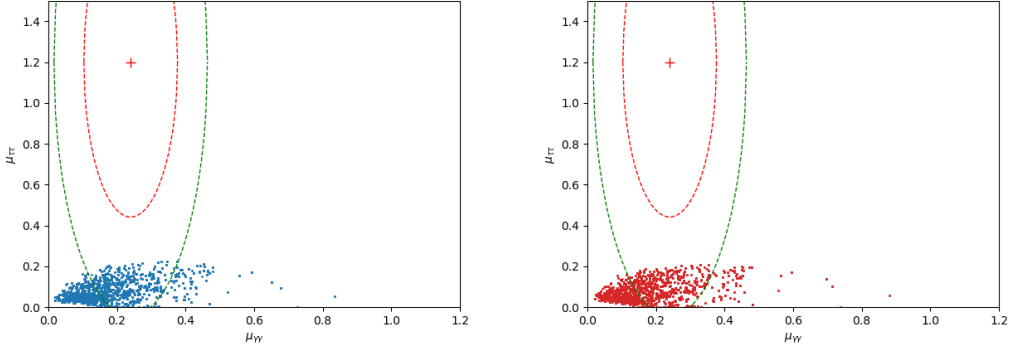


**Figure 1.** Signal strengths  $\mu_{\gamma\gamma}$  and  $\mu_{\tau\tau}$  in the Type-II models with extra fermion contributions in the loop (left) and without them (right).

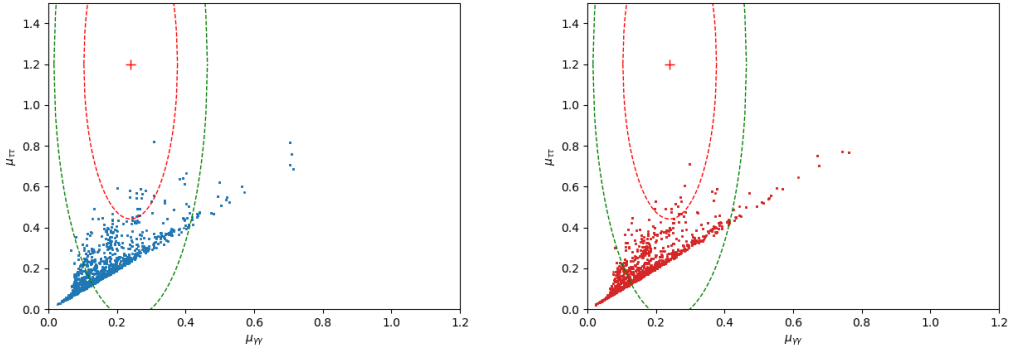


**Figure 2.** Signal strengths  $\mu_{\gamma\gamma}$  and  $\mu_{\tau\tau}$  in the Type-Y models with extra fermion contributions in the loop (left) and without them (right).

quark and lepton are in the ranges of  $0 \leq y_{D,L} \leq 4\pi$ , respectively, but for simplicity we set  $y_D = y_L = 1$ . We note that essential features from the analysis are not modified even though larger Yukawa couplings are chosen. The  $U(1)_H$  gauge coupling must not be large because of constraints from the  $Z'$  boson search at the LHC. We take  $g_X$  to be in the range of  $0.01 \leq g_X \leq 0.1$ . Then, the  $Z'$  mass,  $m_{Z'}$ , is written in terms of the parameters

$$m_{Z'} = \frac{g_H v}{2}, \quad (4.3)$$

where

$$g_H = \sqrt{4g_X^2 \left( \sin^2 \beta + \frac{v_\Phi^2}{v^2} \right)}. \quad (4.4)$$

We find that the  $Z'$  mass is in the range of  $100 \sim 1000$  GeV for allowed parameters while the VEV for the  $U(1)_H$  symmetry breaking is in the range of  $5 \sim 10$  TeV.

## 4.2 Analysis

We perform a scan of 11 parameters in the ranges described in the previous subsection. Then, we apply the theoretical and experimental constraints to the parameter sets and calculate  $\mu_{\gamma\gamma}$ ,  $\mu_{\tau\tau}$  and  $\mu_{bb}$  for those parameters that pass those constraints.

In Fig. 1, we present the signal strengths  $\mu_{\gamma\gamma}$  and  $\mu_{\tau\tau}$  in both Type-II models with extra fermion contributions in the loop (left) and without those contributions (right), respectively. The extra fermion contribution in the loop can especially modify branching ratios of  $\tilde{h} \rightarrow gg$  or  $\gamma\gamma$ . Thus, the production or decay rates of  $\tilde{h}$  can be affected by the extra fermion loop contributions. The two dashed lines denote  $1\sigma$  and  $2\sigma$  regions for the combined experimental values in ATLAS and CMS, respectively. We find that the expectation in our Type-II models is inconsistent with the experiments within  $1\sigma$ , while some points are consistent within  $2\sigma$ . In particular, it is difficult to enhance the  $\mu_{\tau\tau}$  because of effective Yukawa couplings of the 96 GeV scalar boson to the top quarks and tau lepton in the Type-II models:

$$g_{\tilde{h}}^{t,\text{II}} = \frac{\sin \alpha_1 \cos \alpha_2}{\sin \beta}, \quad g_{\tilde{h}}^{\tau,\text{II}} = \frac{\cos \alpha_1 \cos \alpha_2}{\cos \beta}, \quad (4.5)$$

which are normalized to the SM-like Yukawa couplings, respectively. For the  $gg \rightarrow \tilde{h} \rightarrow \tau\tau$  production, both Yukawa couplings are relevant. Then,  $g_{\tilde{h}}^{t,\text{II}}$  is proportional to  $\sin \alpha_1$ , but  $g_{\tilde{h}}^{\tau,\text{II}}$  is to  $\cos \alpha_1$ . Therefore, it would be difficult to enhance both Yukawa couplings for the same  $\alpha_1$ . It turns out that the branching ratio for  $\tilde{h} \rightarrow \tau\tau$  is at most 0.1 in the allowed parameter space, which results in the small signal strength  $\mu_{\tau\tau}$ .

In Fig. 2, we present the signal strengths  $\mu_{\gamma\gamma}$  and  $\mu_{\tau\tau}$  in both Type-Y models with extra fermion contributions in the loop (left) and without those contributions (right), respectively. In these models, the effective Yukawa couplings are given by

$$g_{\tilde{h}}^{t,\text{Y}} = g_{\tilde{h}}^{\tau,\text{Y}} = g_{\tilde{h}}^{t,\text{II}}. \quad (4.6)$$

Because the two effective Yukawa couplings are the same, both production cross sections for  $gg \rightarrow \tilde{h} \rightarrow \gamma\gamma$  and  $gg \rightarrow \tilde{h} \rightarrow \tau\tau$  tend to increase simultaneously as  $\sin \alpha_1$  increases. It turns out that the branching ratio for  $\tilde{h} \rightarrow \tau\tau$  can reach about 0.5 in the allowed parameter space. Then,  $\mu_{\tau\tau}$  can be enhanced compared to the Type-II models and some parameter sets can be consistent with the experimental values within  $1\sigma$ .

In order to find effects of the extra fermions in the loop, we present the signal strengths  $\mu_{\gamma\gamma}$  and  $\mu_{\tau\tau}$  in the Type-Y models with extra fermion-contributions in the loop (blue) and without those contributions (red) in Fig. 3, respectively. Each point corresponds to its own parameter set. Thus, overlapped points means that the contributions from the extra fermions may not be crucial. However, it is apparent that some of blue points are not overlapped with red points and vice versa. The former indicates that the parameter set is consistent with all the experiments, but if the contributions from the extra fermions are ignored, it cannot satisfy one of constraints. The red points which do not overlap with the blue points mean that the parameter set seems to satisfy all constraints without extra fermions. However, if the extra fermion contributions are included, they cannot be candidates for the resonance signals at 96 GeV.

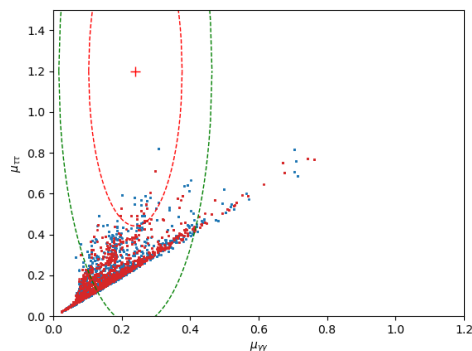


**Figure 3.** Signal strengths  $\mu_{\gamma\gamma}$  and  $\mu_{\tau\tau}$  in the Type-Y models. The blue points correspond to the model including the extra fermions in the loop, while the red ones to the model without their contributions.

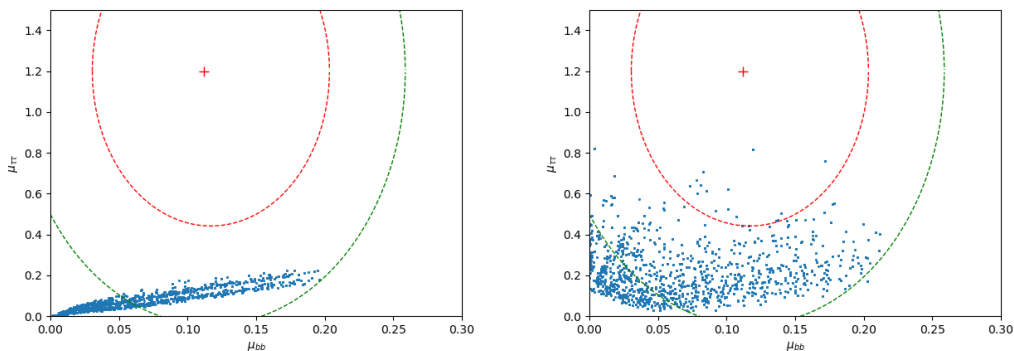


**Figure 4.** Signal strengths  $\mu_{bb}$  and  $\mu_{\tau\tau}$  in the Type-II model (left) and in the Type-Y model (right) with extra fermion contributions in the loop.

In Fig. 4, we present the signal strengths  $\mu_{bb}$  and  $\mu_{\tau\tau}$  in the Type-II model (left) and in the Type-Y model (right) with extra fermion contributions in the loop. The effective couplings of  $\tilde{h}$  to the bottom quark are

$$g_{\tilde{h}}^{b,\text{II}} = g_{\tilde{h}}^{b,\text{Y}} = g_{\tilde{h}}^{\tau,\text{II}}. \quad (4.7)$$

In the Type-II 2HDM, the effective Yukawa coupling,  $g_{\tilde{h}}^{b,\text{II}}$ , of  $\tilde{h}$  to the bottom quark is the same as that to the tau lepton. Thus,  $\mu_{bb}$  tends to be proportional to  $\mu_{\tau\tau}$  as shown in the left figure of Fig. 4. It is obvious that  $\mu_{bb}$  in the Type-II models is preferred to be similarly small like  $\mu_{\tau\tau}$  in the allowed parameter space. On the other hand, in the Type-Y models, the effective Yukawa coupling,  $g_{\tilde{h}}^{b,\text{Y}}$ , of  $\tilde{h}$  to the bottom quark is different from that to the tau quark. As shown in the right figure of Fig. 4, a wider region is allowed in the Type-Y models and some parameters could be within  $1\sigma$  from the central value of the experiments.

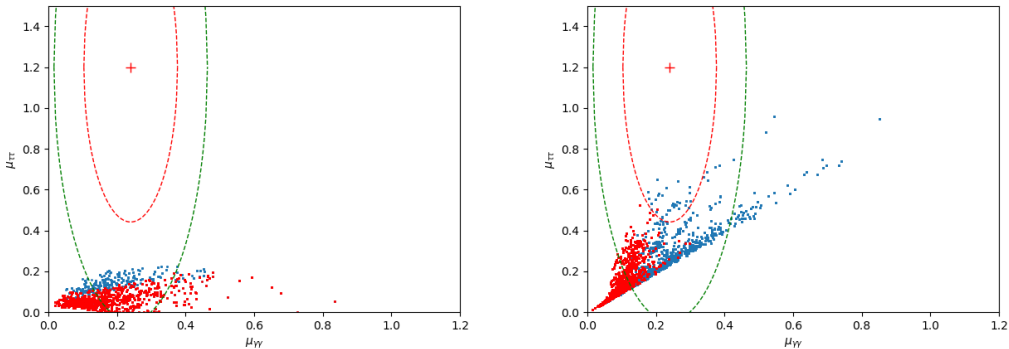


**Figure 5.** Signal strengths  $\mu_{\gamma\gamma}$  and  $\mu_{\tau\tau}$  in the Type-II model (left) and in the Type-Y model (right), respectively. The blue points are the same as those in the left figure of Figs. 1 and 2. The red points satisfy another constraint from  $gg \rightarrow t\bar{t}\tau\tau$  at ATLAS.

### 4.3 Constraints from $t\bar{t}\tau^+\tau^-$ production at the LHC

The 96 GeV scalar boson couples to both the top quark and tau lepton. Thus the production of  $t\bar{t}\tau^+\tau^-$  at the LHC can constrain the scalar boson [65]<sup>1</sup>. Based on the ATLAS Run 2 full data [64], the authors in Ref. [65] have proposed that the Yukawa couplings,  $\rho_{t\bar{t},\tau\tau}^{\tilde{h}}$ , normalized by  $\sqrt{2}$ , should satisfy either

$$\rho_{\tilde{h}}^{tt} = \frac{g_{\tilde{h}}^{t,Y} m_t}{v} < 0.2, \quad (4.8)$$

or

$$\rho_{\tilde{h}}^{\tau\tau} = \frac{g_{\tilde{h}}^{\tau,Y} m_\tau}{v} < 0.002, \quad (4.9)$$

respectively. It is worthwhile to mention that these constraints are based on the analysis of the tree-level calculation for the  $t\bar{t}\tau^+\tau^-$  production [65]. With QCD corrections to the process, the bounds may be slightly modified.

In Fig. 5, we present the signal strengths  $\mu_{\gamma\gamma}$  and  $\mu_{\tau\tau}$  in the Type-II model (left) and in the Type-Y model (right) with extra fermion contributions, respectively. The blue points are the same as those in the left figure of Figs. 1 and 2. The red points satisfy constraints from  $gg \rightarrow t\bar{t}\tau^+\tau^-$  at ATLAS in Eqs. (4.8) and (4.9). In the Type-II case, we find that the constraints from  $gg \rightarrow t\bar{t}\tau^+\tau^-$  do not provide any significant bounds to the model. However, in the Type-Y case, the constraints are very stringent and most of allowed spaces are rejected. It turns out that the allowed region in the Type-Y model is about  $1.3\sigma$  as much as possible. In the Type-II model, the allowed region is about  $1.5\sigma$ , which would be comparable to that in the Type-Y model. Therefore, we find that the Type-Y model is slightly better than the Type-II model to explain the 96 GeV resonances. However, both models are consistent with the resonances within similar statistical errors if the constraints from  $gg \rightarrow t\bar{t}\tau^+\tau^-$  at ATLAS are considered.

<sup>1</sup>See also Ref. [66].

#### 4.4 Benchmark points

We have scanned the parameters, but we see that the allowed parameter range is limited because of the strong constraints, as discussed in Sec. 4.1. In Table 5, we introduce some benchmark points that explicitly show our predictions. Those parameter sets evade the bound from  $t\bar{t}\tau^+\tau^-$ , discussed in Sec. 4.3, and can enhance  $\mu_{\gamma\gamma}$  and  $\mu_{\tau\tau}$ .  $\mu_{bb}$  is within  $2\sigma$  in the cases other than the point 3.

There is no big difference between in the Type-II 2HDM and in the Type-Y 2HDM. The constraints do not allow the mixing among scalars to be large. In fact, the mixing angles,  $\alpha_1$ ,  $\alpha_2$  and  $\alpha_3$ , in all cases, correspond to  $\mathcal{O}(1)|\sin\alpha_{1,2,3}|$ . Then,  $\tilde{h}$ , whose mass is 96 GeV, is dominated by  $h_\Phi$ . The SM-like Higgs boson,  $h$ , dominantly consists of  $h_2$ .  $\tan\beta$  is also small, so that  $|\sin\beta|$  is also  $\mathcal{O}(1)$  and the heavy scalars,  $A$  and  $H$ , mainly consists of  $\chi_1$  and  $h_1$ :  $A \sim \chi_1$  and  $H \sim h_1$ . While  $|\sin\alpha_{1,2,3}|$  and  $|\sin\beta|$  are  $\mathcal{O}(1)$ ,  $|\cos\alpha_{1,2,3}|$  and  $|\cos\beta|$  are at least  $\mathcal{O}(0.1)$  to enhance  $\mu_{\gamma\gamma}$  and  $\mu_{\tau\tau}$ . Thus,  $\tilde{h}$  is approximately expressed as  $\tilde{h} \sim h_\Phi + \mathcal{O}(0.1)h_2$  in the benchmark points. As shown in Table 5,  $g_X$  is very small to evade too large deviation of the  $\rho$  parameter, so the mixing parameters are relevant to the signal strengths. In both cases,  $\mu_{\gamma\gamma}$  and  $\mu_{\tau\tau}$  can be within  $2\sigma$  as shown in Fig. 5, although  $\mu_{\tau\tau}$  in the Type-II 2HDM is smaller than that in the Type-Y 2HDM.

	point 1	point 2	point 3	point 4
Model	Type-II	Type-II	Type-Y	Type-Y
$\alpha_1$	1.35	1.37	1.53	1.46
$\alpha_2$	1.21	1.23	1.34	1.29
$\alpha_3$	4.67	4.65	4.22	4.54
$\tan\beta$	3.20	3.48	1.60	3.28
$v_\Phi$ (GeV)	7350.70	7309.07	5426.80	8894.68
$m_H$ (GeV)	649.56	707.46	645.07	586.47
$m_A$ (GeV)	631.48	694.74	503.50	552.09
$m_{H_\pm}$ (GeV)	649.31	672.13	605.20	601.70
$y_D$	1.0	1.0	1.0	1.0
$y_L$	1.0	1.0	1.0	1.0
$g_X$	$4.76 \times 10^{-2}$	$6.11 \times 10^{-2}$	$4.51 \times 10^{-2}$	$5.65 \times 10^{-2}$
$M_{Z'}$ (GeV)	350.16	446.83	245.08	502.82
$\mu_{bb}$	0.11	$9.75 \times 10^{-2}$	$1.02 \times 10^{-3}$	$2.83 \times 10^{-2}$
$\mu_{\gamma\gamma}$	0.24	0.23	0.20	0.30
$\mu_{\tau\tau}$	0.14	0.13	0.50	0.34

**Table 5.** Benchmark points in the Type-II and Type-Y 2HDMs with  $U(1)_H$  gauge symmetry.

## 5 Summary

We studied the di-photon and di- $\tau$  channels at the LHC as well as the  $b\bar{b}$  channel at LEP, in the Type-II and Type-Y 2HDMs with gauged  $U(1)_H$  symmetry. The  $U(1)_H$  gauge

symmetry distinguishes one Higgs doublet from the other, and naturally suppresses tree-level FCNCs. One extra scalar charged under  $U(1)_H$  is also introduced, so that there are three CP-even neutral scalars at low energy. In our study, the mass of lightest neutral scalar, denoted by  $\tilde{h}$ , was fixed at 96 GeV that corresponds to the mass region where the mild excesses are reported by the ATLAS and CMS collaborations. In our models, extra fermions as well as extra scalars contribute to the di-photon and di- $\tau$  channels. The extra gauge boson deviates  $\rho$  parameter from 1. We surveyed our predictions of the signal strengths,  $\mu_{bb}$ ,  $\mu_{\gamma\gamma}$  and  $\mu_{\tau\tau}$ , scanning parameters. The  $Z'$  couplings are strongly constrained by the  $\rho$  parameter and the  $Z'$  searches, while the contribution of extra fermions affects the signal strengths in some parameter sets. We saw that the dominant contributions to  $\mu_{\gamma\gamma}$  and  $\mu_{\tau\tau}$  are from the mixing among three neutral scalars, not from the extra new fermions. As discussed in Sec. 4, the lightest neutral scalar is mainly composed of the scalar from  $\Phi$ . This result is consistent with the previous work [6]. Our work reveals the underlying theory of the 2HDM with a complex scalar field [6], and explicitly shows how large contributions of the extra fields predicted by extending the symmetry, that distinguishes two Higgs fields, to gauged  $U(1)_H$  symmetry can be. The predictions of the signal strengths, in fact, deviate from them of the 2HDMs without extra fermions. Further study would be required to reveal which setup is preferred by the excesses around 96 GeV.

## Acknowledgments

This work is supported in part by National Research Foundation of Korea (NRF) Grant No. NRF-2018R1A2A3075605 and No. RS-2023-00270569 (S. B.), KIAS Individual Grants under Grant No. PG021403 (P. K.), Grant-in-Aid for Scientific research from the MEXT, Japan, No. 24K07031 (Y. O.), Basic Science Research Program through the National Research Foundation of Korea (NRF) funded by the Ministry of Science, ICT, and Future Planning under the Grant No. NRF-2021R1A2C2011003m and RS-2023-00237615 (C. Y.).

## A Bounded-from-below condition

We present constraints from the condition for scalar potential to be bounded from below. For the derivation of the constraints, we follow the method derived in Ref. [57, 58]. The quartic couplings are constrained by

$$\lambda_{1,2,\Phi} > 0, \quad \lambda_3 + (\lambda_4 \pm \lambda_4)/2 + 2\sqrt{\lambda_1\lambda_2} > 0, \quad \tilde{\lambda}_{1,2} + 2\sqrt{\lambda_{1,2}\lambda_\Phi} > 0 \quad (\text{A.1})$$

together with the following four conditions as follows

$$\begin{aligned} & [(\lambda_3 > 0 \cap \lambda_{34} > 0) \cup (E_1)] \cap [(\tilde{\lambda}_1 > 0) \cup (4\lambda_1\lambda_\Phi - \tilde{\lambda}_1^2 > 0)] \\ & \cap [(\tilde{\lambda}_2 > 0) \cup (4\lambda_2\lambda_\Phi - \tilde{\lambda}_2^2 > 0)] \cap [(\tilde{\lambda}_1 > 0 \cap \tilde{\lambda}_2 > 0) \cup (E_2)], \end{aligned} \quad (\text{A.2})$$

where

$$\begin{aligned} E_1 &= [\lambda_{12}^2 - \lambda_3^2 > 0] \cap [\lambda_{12}^2 - \lambda_{34}^2 > 0] \cap [\lambda_{12}^2 - \lambda_3\lambda_{34} + \sqrt{(\lambda_{12}^2 - \lambda_3^2)(\lambda^2 - \lambda_{34}^2)} > 0], \quad (\text{A.3}) \\ E_2 &= [\lambda_{1\Phi}^2 - \tilde{\lambda}_1^2 > 0] \cap [\lambda_{2\Phi}^2 - \tilde{\lambda}_2^2 > 0] \cap [2(\lambda_3 + D)\lambda_\Phi - \tilde{\lambda}_1\tilde{\lambda}_2 + \sqrt{(\lambda_{1\Phi}^2 - \tilde{\lambda}_1^2)(\lambda_{2\Phi}^2 - \tilde{\lambda}_2^2)} > 0] \end{aligned}$$



Here,

$$\lambda_{12}^2 = 4\lambda_1\lambda_2, \quad \lambda_{1\Phi}^2 = 4\lambda_1\lambda_\Phi, \quad \lambda_{2\Phi}^2 = 4\lambda_2\lambda_\Phi, \quad (\text{A.5})$$

$$D = \min(\lambda_4, 0). \quad (\text{A.6})$$

## B Effective couplings

In this appendix, we present the definition of the effective couplings for the triple vertices of gauge bosons and scalar bosons. The effective couplings are defined by the couplings for the triple vertices normalized by those in the SM

$$g_{W^\pm H^\mp A} = (V_A)_{33} \cos \beta - (V_A)_{32} \sin \beta, \quad (\text{B.1})$$

$$g_{W^\pm H^\mp S_i} = (R)_{i2} \cos \beta - (R)_{i1} \sin \beta, \quad (\text{B.2})$$

$$\begin{aligned} g_{ZAS_i} &= \cos \theta [(R)_{i1}(V_A)_{32} + (R)_{i2}(V_A)_{33}] \\ &\quad - \frac{2g_X}{g_2} \sin \theta [(R)_{i2}(V_A)_{33} - (R)_{i3}(V_A)_{31}], \end{aligned} \quad (\text{B.3})$$

$$\begin{aligned} g_{ZZS_i} &= \cos^2 \theta [(R)_{i1} \cos \beta + (R)_{i2} \sin \beta] - \frac{4c_W^2 g_X^2}{g_2^2} \sin \theta (R)_{i2} \sin \beta \\ &\quad + \frac{4c_W^2 g_X^2}{g_2^2} \sin^2 \theta \left[ (R)_{i2} \sin \beta + (R)_{i3} \frac{v_\Phi}{v} \right], \end{aligned} \quad (\text{B.4})$$

$$\begin{aligned} g_{ZZ'S_i} &= \frac{2c_W g_X}{g_2} (R)_{i2} \sin \beta (\cos^2 \theta - \sin^2 \theta) \\ &\quad + \frac{\sin 2\theta}{2} \left[ (R)_{i1} \cos \beta + (R)_{i2} \sin \beta + \frac{4c_W^2 g_X^2}{g_2^2} \left\{ (R)_{i2} \sin^2 \beta + \frac{v_\Phi}{v} (R)_{i3} \right\} \right] \end{aligned} \quad (\text{B.5})$$

$$g_{WWS_i} = (R)_{i1} \cos \beta + (R)_{i2} \sin \beta, \quad (\text{B.6})$$

$$g_{W^\pm H^\mp Z} = \frac{g_X}{g_2} \sin \theta \sin 2\beta, \quad (\text{B.7})$$

$$g_{W^\pm H^\mp Z'} = -\frac{g_X}{g_2} \cos \theta \sin 2\beta, \quad (\text{B.8})$$

where  $S_i \equiv (\tilde{h}, h, H)$ .

## References

- [1] G. Aad *et al.* [ATLAS], Phys. Lett. B **716**, 1-29 (2012) [arXiv:1207.7214 [hep-ex]].
- [2] S. Chatrchyan *et al.* [CMS], Phys. Lett. B **716**, 30-61 (2012) [arXiv:1207.7235 [hep-ex]].
- [3] A. M. Sirunyan *et al.* [CMS], Phys. Lett. B **793**, 320-347 (2019) [arXiv:1811.08459 [hep-ex]].
- [4] CMS collaboration, Tech. Rep. CMS-HIG-20-002 (2023).
- [5] C. Arcangeletti, ATLAS, *LHC Seminar*, [indico.cern.ch](https://indico.cern.ch), 2023.
- [6] T. Biekötter, S. Heinemeyer and G. Weiglein, Phys. Rev. D **109**, no.3, 3 (2024) [arXiv:2306.03889 [hep-ph]].
- [7] A. Tumasyan *et al.* [CMS], JHEP **07**, 073 (2023) [arXiv:2208.02717 [hep-ex]].

- [8] J. Cao, X. Guo, Y. He, P. Wu and Y. Zhang, Phys. Rev. D **95**, no.11, 116001 (2017) [arXiv:1612.08522 [hep-ph]].
- [9] A. Azatov, R. Contino and J. Galloway, JHEP **04**, 127 (2012) [erratum: JHEP **04**, 140 (2013)] [arXiv:1202.3415 [hep-ph]].
- [10] T. Biekötter, M. Chakraborti and S. Heinemeyer, Eur. Phys. J. C **80**, no.1, 2 (2020) [arXiv:1903.11661 [hep-ph]].
- [11] T. Biekötter, M. Chakraborti and S. Heinemeyer, PoS **CORFU2018**, 015 (2019) [arXiv:1905.03280 [hep-ph]].
- [12] T. Biekötter, M. Chakraborti and S. Heinemeyer, Int. J. Mod. Phys. A **36**, no.22, 2142018 (2021) [arXiv:2003.05422 [hep-ph]].
- [13] T. Biekötter, A. Grohsjean, S. Heinemeyer, C. Schwanenberger and G. Weiglein, Eur. Phys. J. C **82**, no.2, 178 (2022) [arXiv:2109.01128 [hep-ph]].
- [14] S. Heinemeyer, C. Li, F. Lika, G. Moortgat-Pick and S. Paasch, Phys. Rev. D **106**, no.7, 075003 (2022) [arXiv:2112.11958 [hep-ph]].
- [15] T. Biekötter, S. Heinemeyer and G. Weiglein, JHEP **08**, 201 (2022) [arXiv:2203.13180 [hep-ph]].
- [16] T. Biekötter, S. Heinemeyer and G. Weiglein, Phys. Lett. B **846**, 138217 (2023) [arXiv:2303.12018 [hep-ph]].
- [17] S. Bhattacharya, G. Coloretti, A. Crivellin, S. E. Dahbi, Y. Fang, M. Kumar and B. Mellado, [arXiv:2306.17209 [hep-ph]].
- [18] S. Banik, G. Coloretti, A. Crivellin and B. Mellado, [arXiv:2312.01458 [hep-ph]].
- [19] A. Kundu, S. Maharana and P. Mondal, Nucl. Phys. B **955**, 115057 (2020) [arXiv:1907.12808 [hep-ph]].
- [20] J. Cao, X. Jia, Y. Yue, H. Zhou and P. Zhu, Phys. Rev. D **101**, no.5, 055008 (2020) [arXiv:1908.07206 [hep-ph]].
- [21] A. A. Abdelalim, B. Das, S. Khalil and S. Moretti, Nucl. Phys. B **985**, 116013 (2022) [arXiv:2012.04952 [hep-ph]].
- [22] A. Belyaev, R. Benbrik, M. Boukidi, M. Chakraborti, S. Moretti and S. Semlali, JHEP **05**, 209 (2024) [arXiv:2306.09029 [hep-ph]].
- [23] J. A. Aguilar-Saavedra, H. B. Câmara, F. R. Joaquim and J. F. Seabra, Phys. Rev. D **108**, no.7, 075020 (2023) [arXiv:2307.03768 [hep-ph]].
- [24] J. Dutta, J. Lahiri, C. Li, G. Moortgat-Pick, S. F. Tabira and J. A. Ziegler, Eur. Phys. J. C **84**, no.9, 926 (2024) [arXiv:2308.05653 [hep-ph]].
- [25] U. Ellwanger and C. Hugonie, Eur. Phys. J. C **83**, no.12, 1138 (2023) [arXiv:2309.07838 [hep-ph]].
- [26] J. Cao, X. Jia, J. Lian and L. Meng, Phys. Rev. D **109**, no.7, 075001 (2024) [arXiv:2310.08436 [hep-ph]].
- [27] G. Arcadi, G. Busoni, D. Cabo-Almeida and N. Krishnan, [arXiv:2311.14486 [hep-ph]].
- [28] A. T. Mulaudzi, M. Kumar, A. Goyal and B. Mellado, [arXiv:2312.08807 [hep-ph]].

- [29] C. X. Liu, Y. Zhou, X. Y. Zheng, J. Ma, T. F. Feng and H. B. Zhang, *Phys. Rev. D* **109**, no.5, 056001 (2024) [arXiv:2402.00727 [hep-ph]].
- [30] J. Cao, X. Jia and J. Lian, [arXiv:2402.15847 [hep-ph]].
- [31] J. Kalinowski and W. Kotlarski, *JHEP* **07**, 037 (2024) [arXiv:2403.08720 [hep-ph]].
- [32] U. Ellwanger and C. Hugonie, *Eur. Phys. J. C* **84**, no.5, 526 (2024) [arXiv:2403.16884 [hep-ph]].
- [33] U. Ellwanger, C. Hugonie, S. F. King and S. Moretti, *Eur. Phys. J. C* **84**, no.8, 788 (2024) [arXiv:2404.19338 [hep-ph]].
- [34] A. Arhrib, K. H. Phan, V. Q. Tran and T. C. Yuan, [arXiv:2405.03127 [hep-ph]].
- [35] R. Benbrik, M. Boukidi and S. Moretti, [arXiv:2405.02899 [hep-ph]].
- [36] J. Lian, [arXiv:2406.10969 [hep-ph]].
- [37] A. Khanna, S. Moretti and A. Sarkar, [arXiv:2409.02587 [hep-ph]].
- [38] B. Ait-Ouazghour, M. Chabab and K. Goure, [arXiv:2410.11140 [hep-ph]].
- [39] S. Ashanujjaman, S. Banik, G. Coloretti, A. Crivellin, B. Mellado and A. T. Mulaudzi, *Phys. Rev. D* **108**, no.9, L091704 (2023) [arXiv:2306.15722 [hep-ph]].
- [40] S. Banik, G. Coloretti, A. Crivellin and B. Mellado, [arXiv:2308.07953 [hep-ph]].
- [41] G. Coloretti, A. Crivellin and B. Mellado, *Phys. Rev. D* **110**, no.7, 073001 (2024) [arXiv:2312.17314 [hep-ph]].
- [42] Y. Dong, K. Wang and J. Zhu, [arXiv:2410.13636 [hep-ph]].
- [43] D. Borah, S. Mahapatra, P. K. Paul and N. Sahu, *Phys. Rev. D* **109**, no.5, 055021 (2024) [arXiv:2310.11953 [hep-ph]].
- [44] A. Ahriche, M. L. Bellilet, M. O. Khojali, M. Kumar and A. T. Mulaudzi, *Phys. Rev. D* **110**, no.1, 015025 (2024) [arXiv:2311.08297 [hep-ph]].
- [45] A. Ahriche, *Phys. Rev. D* **110**, no.3, 3 (2024) [arXiv:2312.10484 [hep-ph]].
- [46] T. K. Chen, C. W. Chiang, S. Heinemeyer and G. Weiglein, *Phys. Rev. D* **109**, no.7, 075043 (2024) [arXiv:2312.13239 [hep-ph]].
- [47] P. S. B. Dev, R. N. Mohapatra and Y. Zhang, *Phys. Lett. B* **849**, 138481 (2024) [arXiv:2312.17733 [hep-ph]].
- [48] K. Wang and J. Zhu, *Chin. Phys. C* **48**, no.7, 073105 (2024) doi:10.1088/1674-1137/ad4268 [arXiv:2402.11232 [hep-ph]].
- [49] S. Yaser Ayazi, M. Hosseini, S. Paktinat Mehdiabadi and R. Rouzbehi, *Phys. Rev. D* **110**, no.5, 055004 (2024) [arXiv:2405.01132 [hep-ph]].
- [50] S. L. Glashow and S. Weinberg, *Phys. Rev. D* **15**, 1958 (1977) doi:10.1103/PhysRevD.15.1958
- [51] P. Ko, Y. Omura and C. Yu, *Phys. Lett. B* **717**, 202-206 (2012) [arXiv:1204.4588 [hep-ph]].
- [52] P. Ko, Y. Omura and C. Yu, *JHEP* **01**, 016 (2014) [arXiv:1309.7156 [hep-ph]].
- [53] P. Ko, Y. Omura and C. Yu, *JHEP* **11**, 054 (2014) [arXiv:1405.2138 [hep-ph]].
- [54] P. Ko, Y. Omura and C. Yu, *JHEP* **06**, 034 (2015) [arXiv:1502.00262 [hep-ph]].
- [55] D. W. Jung, K. Y. Lee and C. Yu, *Phys. Rev. D* **108**, no.9, 095002 (2023) doi:10.1103/PhysRevD.108.095002 [arXiv:2305.18740 [hep-ph]].

- [56] A. Arhrib, R. Benbrik, M. Chabab, G. Moulhaka, M. C. Peyranere, L. Rahili and J. Ramadan, *Phys. Rev. D* **84**, 095005 (2011) [arXiv:1105.1925 [hep-ph]].
- [57] J. Horejsi and M. Kladiva, *Eur. Phys. J. C* **46**, 81-91 (2006) doi:10.1140/epjc/s2006-02472-3 [arXiv:hep-ph/0510154 [hep-ph]].
- [58] M. Muhlleitner, M. O. P. Sampaio, R. Santos and J. Wittbrodt, *JHEP* **03**, 094 (2017) [arXiv:1612.01309 [hep-ph]].
- [59] W. Grimus, L. Lavoura, O. M. Ogreid and P. Osland, *J. Phys. G* **35**, 075001 (2008) [arXiv:0711.4022 [hep-ph]].
- [60] R. L. Workman *et al.* [Particle Data Group], *PTEP* **2022**, 083C01 (2022).
- [61] A. Arbey, F. Mahmoudi, O. Stal and T. Stefaniak, *Eur. Phys. J. C* **78**, no.3, 182 (2018) [arXiv:1706.07414 [hep-ph]].
- [62] P. Bechtle, D. Dercks, S. Heinemeyer, T. Klingl, T. Stefaniak, G. Weiglein and J. Wittbrodt, *Eur. Phys. J. C* **80**, no.12, 1211 (2020) [arXiv:2006.06007 [hep-ph]]; P. Bechtle, O. Brein, S. Heinemeyer, O. Stål, T. Stefaniak, G. Weiglein and K. E. Williams, *Eur. Phys. J. C* **74**, no.3, 2693 (2014) [arXiv:1311.0055 [hep-ph]].
- [63] P. Bechtle, S. Heinemeyer, T. Klingl, T. Stefaniak, G. Weiglein and J. Wittbrodt, *Eur. Phys. J. C* **81**, no.2, 145 (2021) [arXiv:2012.09197 [hep-ph]]; P. Bechtle, S. Heinemeyer, O. Stål, T. Stefaniak and G. Weiglein, *Eur. Phys. J. C* **74**, no.2, 2711 (2014) [arXiv:1305.1933 [hep-ph]].
- [64] G. Aad *et al.* [ATLAS], *JHEP* **08**, 175 (2022) [arXiv:2201.08269 [hep-ex]].
- [65] S. Iguro, T. Kitahara and Y. Omura, *Eur. Phys. J. C* **82**, no.11, 1053 (2022) [arXiv:2205.03187 [hep-ph]].
- [66] S. Iguro, T. Kitahara, Y. Omura and H. Zhang, *Phys. Rev. D* **107**, no.7, 075017 (2023) [arXiv:2211.00011 [hep-ph]].